Published in IET Communications
Received on 22nd December 2012
Revised on 9th May 2013
Accepted on 3rd June 2013
doi: 10.1049/iet-com.2012.0806

ISSN 1751-8628

An efficient multiple access interference suppression scheme in asynchronous femtocells

Behrouz Banitalebi, Jamshid Abouei

Department of Electrical and Computer Engineering, Yazd University, Yazd, Iran
E-mail: abouei@yazd.ac.ir

Abstract: This work considers a code division multiple access (CDMA)-based femtocell system where a fixed set of subscribed users communicate simultaneously to a femtocell access point (FAP) in an asynchronous fashion during the uplink. The main goal of this paper is to present an augmentation protocol for the physical layer of the CDMA2000 femtocell standard with focus on the multiple access interference (MAI) suppression. The above-closed access femtocell uses a unique set of cyclic orthogonal binary codes to eliminate the MAI caused by packet collisions. This property ensures that the time and data rate asynchronicity of active nodes in a femtocell produces a zero MAI situation at the FAP. The work investigates the optimality and the effectiveness of such codes in femtocells from the link bit error rate performance in a practical Rayleigh-fading environment, where Kalman filtering is used at the FAP for the channel estimation. Theoretical findings are verified by simulation evaluations and it is shown numerically a significant improvement in the performance of the proposed scheme when compared with conventional non-cyclic orthogonal codes in a Rayleigh-fading channel in the asynchronous femtocell.

Nomenclature

Throughout this paper, we use normal letters for scalars. Boldface lower case and capital letters denote vectors and matrices, respectively. The transposition and the conjugated transposition of a complex matrix $\boldsymbol{A}$ are denoted by $\boldsymbol{A}^{\mathrm{T}}$ and $\boldsymbol{A}'$, respectively. $\mathbb{E}[.]$ represents the expectation operator and for the signal s_i, the decoded or estimated signal is represented by $\hat{s}_i$. Also, $\boldsymbol{I}_{L\times L}$ is an $L\times L$ identity matrix, and $\mathbf{O}_{L\times L}$ is an all zero matrix. Finally, the dot or inner product of two vectors $\boldsymbol{x}=[x_1,\ldots,x_n]$ and $\boldsymbol{y}=[y_1,\ldots,y_n]$ is defined as $\boldsymbol{x}\cdot\boldsymbol{y}=\sum_{i=1}^{n}x_iy_i$.

1 Introduction

The femtocell concept has been emerged as a new short range technology in the next generation of wireless cellular networks, creating the benefits of higher capacity, indoor coverage enhancement and offload traffic from existing macrocellular networks [1, 2]. A femtocell is a small wireless access point typically used in residential or small business environments, where signals from outdoor cells have difficulty reaching mobile phone users. In recent years, several research works have addressed the key technical challenges in femtocell networks from different perspectives, including open/closed access deployment [3], capacity/coverage area [4, 5], power control [6] and interference management [7–11]. Central to the study of key designs in the physical layer of femtocell networks is to control the interference since it directly affects the quality of service of the network such as the bit error rate (BER) or the throughput. In such networks, the RF interference can be in the form of the cross-tier interference between femtocells and macrocells, the interference between femtocells, and the interference observed at the femtocell access point (FAP) because of the simultaneous transmission of the nodes in each femtocell over the same frequency band. It is shown that the femtocell-to-femtocell interference is relatively small due to the low transmission power and penetration losses [2]. Park *et al.* [7] adopt a macrocell beam subset selection strategy to reduce the cross-tier interference in two-tier femtocell networks and in effect to maximise the throughput of the macrocell. Jo *et al.* [8] propose an open-loop approach and a closed-loop control scheme for the maximum transmit power of femtocell users to suppress the cross-tier interference. The authors in [9] present an efficient power control scheme combined with the orthogonal frequency division multiple access (OFDMA) technique to control the femtocell-to-macrocell interference and vice versa. The authors in [12] provide a survey on the different interference and resource management techniques in femtocell self-organising networks according to specific classification criteria. These techniques are derived from power control, proper cell planning, frequency reuse, OFDMA, self-configuration and self-optimisation. The adaptation of femtocells to their surrounding environments and spectrum allocations in the presence of intra and the cross-tier interference through deploying the OFDMA macro/femtocell scenario are provided in [13]. In [14], the

authors develop the channel-gain oriented and the minimum interference channel selection schemes to tackle the femtocell interference problem.

Most of the work on the interference management in femtocells has been focused on the cross-tier interference avoidance. Of interest is the use of efficient schemes in controlling the multiple access interference (MAI) observed at the FAP because of the uplink transmission of active nodes in each femtocell operating in the same frequency band. In this paper, we address this issue and assume that other interferences from different sources are controlled by the orthogonal signaling (e.g. time or frequency) in the network [9]. On the other hand, devices in upcoming femtocells for next generation of wireless networks should communicate with their FAPs for uninterrupted voice calls, clear video images, online games and fast uploads and downloads. In such femtocell structures having various wireless devices with different active mode durations as well as different data rates introduce the time and the data rate asynchronicity. When multiple devices in a femtocell access a common frequency band with such an asynchronicity existent, the FAP experiences the packet collision. Another challenge comes from the intersymbol interference occurred in an indoor femtocell environment due to the multipath-fading phenomenon. In fact, owing to the reflection, refraction and scattering of radio waves by structures and furnishes inside a femtocell, the transmitted signal most often reaches the FAP by more than one path, resulting in a phenomenon known as multipath fading. The multipath event causes the deep fading and the pulse spreading of the signal, hence the intersymbol interference can be caused in a femtocell system. The direct sequence code division multiple access (DS-CDMA) physical layer scheme is the most promising for use in femtocells [10, 15], since it meets the following requirements: (i) collision-free, (ii) multipath resilient properties, (iii) supports various data rates, and (iv) uses the available frequency and time resources efficiently [16].

Motivated by the above considerations, this paper addresses a CDMA-based closed access femtocell where a fixed set of subscribed users communicate simultaneously to an FAP in an asynchronous fashion during the uplink. The main goal of this paper is to present an augmentation protocol for the physical layer of the CDMA2000 femtocell standard [17] with emphasis on the MAI cancellation. The focus of the present protocol is to introduce and analyse an efficient set of cyclic orthogonal binary codes to eliminate the MAI caused by packet collisions. This property ensures that the time and the data rate asynchronicity of active devices in a femtocell do not produce the MAI at the FAP. The work investigates the optimality and the effectiveness of such codes in femtocells from the link BER performance in an additive white Gaussian noise (AWGN) channel and also a practical Rayleigh-fading environment. In view of the practical implementation, Kalman filtering is used at the FAP for the channel estimation to track a simple Gauss–Markov channel [18]. Our analysis is supported with some Monte Carlo (MC) simulation results to show a significant improvement in the performance of the proposed scheme when compared with conventional non-cyclic orthogonal codes in an AWGN/Rayleigh-fading channel. The proposed protocol is capable of robustly protecting the performance of all the active nodes in femtocell networks from the MAI points of view, and in effect increases the Shannon capacity of the femtocell system.

The rest of the paper is organised as follows. In Section 2, a femtocell system model and the objective of this paper are described. An efficient set of cyclic orthogonal binary codes is introduced, analysed and discussed in Section 3. Section 4 provides simulation evaluations, experimental with synthetic results and interpretation of the findings. To complete the evaluation of the proposed protocol, the BER performance of our scheme using Kalman filtering is examined in Section 4. Finally in Section 5, an overview of the results and conclusions are presented.

2 Femtocell system description

In this work, we consider a CDMA-based closed access femtocell system consisting of K registered wireless devices denoted by $U_1, U_2, \ldots, U_K$ communicating to the femto access point AP (Fig. 1). In fact, the AP only provides service to specified subscribers in closed access, to ensure they can monopolise their own femtocell and its backhaul with privacy and security [2, 3]. It is assumed that each U_i, $i = 1, \ldots, K$, transmits its packets in a single-hop setting to the AP. To keep the complexity of communication hardware as low as possible, we assume that all the devices U_i's transmit data over the same frequency band. For such an uplink multiple access transmission, the AP faces the MAI from the devices inside the femtocell. We assume that the cross-tier interferences from different sources such as macrocells or other femtocells are controlled by the orthogonal signalling in the network such as time or frequency [9, 13].

For the proposed CDMA-based femtocell system, the bit stream of each U_i with the bit duration T_b is directly multiplied by a preassigned cyclic orthogonal code (as described in Section 3) with the chip duration T_c and the processing gain $N \triangleq T_b/T_c$. It is assumed that N is fixed for all U_i's. The length of cyclic orthogonal codes is a function of different parameters such as the number of devices in the femtocell, the available spectrum, and the targeted performance of the system. The necessary condition to avoid the MAI in the described system is to choose the length of $N = 2^k$ such that $K \leq k + 1$, as we will prove in Theorem 1 in Section 3. Clearly, K is a small value for a femtocell when compared with the number of nodes in classical cellular systems or picocells. Note that in our scenario, we do not need to deploy a long scrambling

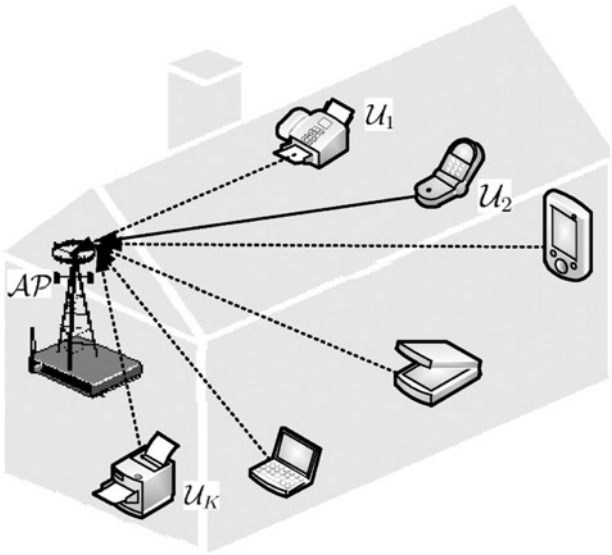

Fig. 1 *Uplink transmission in a closed access femtocell*

doi: 10.1049/iet-com.2012.0806

code due to the fact that we are using a low number of femto user equipments (fues) in each femtocell. It is worth mentioning that the length of the short scrambling codes used in spread spectrum systems is equal to 256 chips [19]. In this case, there are $K = k + 1 = 9$ cyclic orthogonal codes. Therefore because of the low number of 'fues', short scrambling code could be applied to the FAPs and that is enough for the separation of neighbouring femtocells.

Denoting $s_i(n)$ as the transmitted signal from U_i at time n, the received signal at the AP is given by

$$r(n) = \sum_{i=1}^{K} \sum_{j=1}^{L} \alpha_{ij}(n) s_i\left(n - \tau_{ij}\right) w_i + z(n) \tag{1}$$

where $\alpha_{ij}(n)$ and τ_{ij} are the jth channel tap coefficients and their corresponding delays between the device U_i and the AP, respectively, L is the maximum number of channel taps, w_i is the preassigned cyclic orthogonal code of node U_i, and $z(n)$ is an AWGN. It should be noted that the indoor environment in which the proposed femtocell operates involves many obstacles (i.e. wall, furniture, etc.), which leads to the reduced line-of-sight (LOS). This behaviour suggests a Rayleigh-fading channel for the above femtocell model, thus for a such channel, $\alpha_{ij}(n)$'s are modelled as complex Gaussian random variables.

To decode an arbitrary signal $s_\ell(n)$, $\ell = 1, ..., K$, at the femto access point AP, the model simply despreads $r(n)$ in (1) with the code w_ℓ associated with $s_\ell(n)$ as follows

$$\hat{s}_\ell(n) = \sum_{j=1}^{L} \alpha_{\ell j}(n) s_\ell(n - \tau_{\ell j}) w_\ell^2 + \sum_{\substack{i=1 \\ i \neq \ell}}^{K} \sum_{j=1}^{L} \alpha_{ij}(n) s_i(n - \tau_{ij}) w_i w_\ell + w_\ell z(n), \quad \ell = 1, ..., K, \tag{2}$$

where by definition w_ℓ^2 will equal to one. Assuming that the AP utilises a single user detection, the second term in (2) introduces the MAI in the system. Since, the MAI is affected by the spreading codes w_i, selecting pseudo-noise codes with the minimum cross-correlation property is a crucial task in designing CDMA-based femtocells. It is shown that Walsh–Hadamard codes display 'perfectly 'zero' cross-correlation' or equivalently a MAI-free situation in '*synchronous*' communication scenarios. However, in a real femtocell environment where multiple wireless devices experience different active mode durations and data rates, the time and the data rate asynchronicity are imposed on such a femtocell system. Thus, the main problem in using Walsh–Hadamard codes is the loss of orthogonality because of such MAC/PHY layers asynchronicity, and/or the multipath signal propagation. Motivated by the above consideration, the focus of the next section is to introduce and analyse an efficient protocol using 'cyclic orthogonal codes' that eliminate the MAI in a such asynchronous CDMA-based femtocell with multipath-fading effects.

3 Cyclic orthogonality of Hadamard codes

Walsh–Hadamard codes have been widely used in DS-CDMA communications. Inherently, the codes generated from the rows or columns of the Walsh–Hadamard matrix $\boldsymbol{H}_{2^k}$, $k \geq 1$, known as classical Walsh–Hadamard codes, are mutually orthogonal in the zero phase shift. The Walsh–Hadamard matrix is a special matrix of size $N \times N$, where $N = 2^k$ is a power of 2. Setting $\boldsymbol{H}_1 = [1]$, a higher dimensional Hadamard matrix $\boldsymbol{H}_{2^k}$, $k \geq 1$, is iteratively generated as

$$\boldsymbol{H}_{2^k} = \begin{bmatrix} \boldsymbol{H}_{2^{k-1}} & \boldsymbol{H}_{2^{k-1}} \\ \boldsymbol{H}_{2^{k-1}} & -\boldsymbol{H}_{2^{k-1}} \end{bmatrix} = \boldsymbol{H}_2 \otimes \boldsymbol{H}_{2^{k-1}},$$

where $\otimes$ denotes the Kronecker product [20]. The orthogonality property of the Walsh–Hadamard codes is lost if the codes are phase shifted as shown in [21]. To address this issue, let denote $\boldsymbol{W}(2^k, k)$ as the set of all 2^k codes generated from the matrix $\boldsymbol{H}_{2^k}$, $k \geq 1$. We assume the Walsh–Hadamard codes $\boldsymbol{w}_i^{(k)} \in \boldsymbol{W}(2^k, k)$ are indexed by $i = 1,2, \ldots, 2^k$, where $\boldsymbol{w}_i^{(k)} \triangleq \left(w_{i,1}, \ldots, w_{i,2^k}\right)$ with the length $N = 2^k$. We define $\boldsymbol{w}_i^{(k)}(\xi)$ as the ξth right circular shifted version of the periodic Walsh–Hadamard code $\boldsymbol{w}_i^{(k)}$ where each single time shift is equal to the chip duration T_c. Without loss of generality and for ease of our analysis, we assume $T_c = 1$. In this case, the discrete-time periodic cross-correlation between any arbitrary distinct pair of $\boldsymbol{w}_i^{(k)}$, $\boldsymbol{w}_j^{(k)} \in \boldsymbol{W}(2^k, k)$, $i \neq j$, with the phase shift $\tau = 0,1, \ldots, 2^k - 1$, is defined as the following inner product [16]

$$R_{\boldsymbol{w}_i^{(k)} \boldsymbol{w}_j^{(k)}}(\tau) \triangleq \boldsymbol{w}_i^{(k)}(\tau + \xi) \cdot \boldsymbol{w}_j^{(k)}(\xi) \tag{3}$$

Ideally, we would like $R_{\boldsymbol{w}_i^{(k)} \boldsymbol{w}_j^{(k)}}(\tau)$ in (3) to be zero for all possible $\tau = 0,1, \ldots, 2^k - 1$. For the case of synchronous CDMA-based femtocells, where $\tau = 0$, the MAI at the AP will be cancelled because of the $R_{\boldsymbol{w}_i^{(k)} \boldsymbol{w}_j^{(k)}}(0) = 0$ which comes from the mutual orthogonality of the classical Walsh–Hadamard codes generated from the rows of $\boldsymbol{H}_{2^k}$. However, for an asynchronous CDMA-based femtocell, there is a performance penalty with respect to the synchronised case due to the loss of orthogonality between the classical Walsh–Hadamard codes. In fact, for any arbitrary distinct pair of Walsh–Hadamard codes, the cross-correlation $R_{\boldsymbol{w}_i^{(k)} \boldsymbol{w}_j^{(k)}}(\tau)$ for each phase shift $\tau > 0$ 'is not necessarily zero'. Fig. 2 deals with this issue and shows that the cross-correlation between the codes of $\boldsymbol{W}(64,6)$ at the first and second phase shifts. We see from Fig. 2 that only 'some' codes exhibit the zero cross-correlation situation. We are particularly interested in these sets of codes for using in our femtocell system model. When examined, we can find a set of $K = 7$ codes from the $\boldsymbol{W}(64,6)$ that have zero cross-correlation in all phase shifts $\tau = 0,1, \ldots, 63$. This property of Walsh–Hadamard codes was evaluated 'numerically' for the first time in [21] and then in [22, 23] for $1 \leq k \leq 10$ without any mathematical proof. As shown numerically in [21], among 2^k Walsh–Hadamard codes $\boldsymbol{W}(2^k, k)$, there exists a subset of $k + 1$ codes belong to $\boldsymbol{W}(2^k, k)$ denoted by $\widetilde{\boldsymbol{W}}^{(k)} \triangleq \left\{\widetilde{\boldsymbol{w}}_1^{(k)}, \ldots, \widetilde{\boldsymbol{w}}_{k+1}^{(k)}\right\}$ with this property that the cross-correlation of any arbitrary distinct pair of Walsh–Hadamard codes in $\widetilde{\boldsymbol{W}}^{(k)}$ is zero for every value of the phase shift $\tau = 0,1, \ldots, 2^k - 1$. We prove analytically this proposition in the next theorem.

Theorem 1: Among 2^k Walsh–Hadamard codes $\boldsymbol{W}(2^k, k)$, there exists a subset of $k + 1$ codes with this property that the cross-correlation of any arbitrary distinct pair of these codes is zero for every value of $\tau = 0,1,...,2^k - 1$.

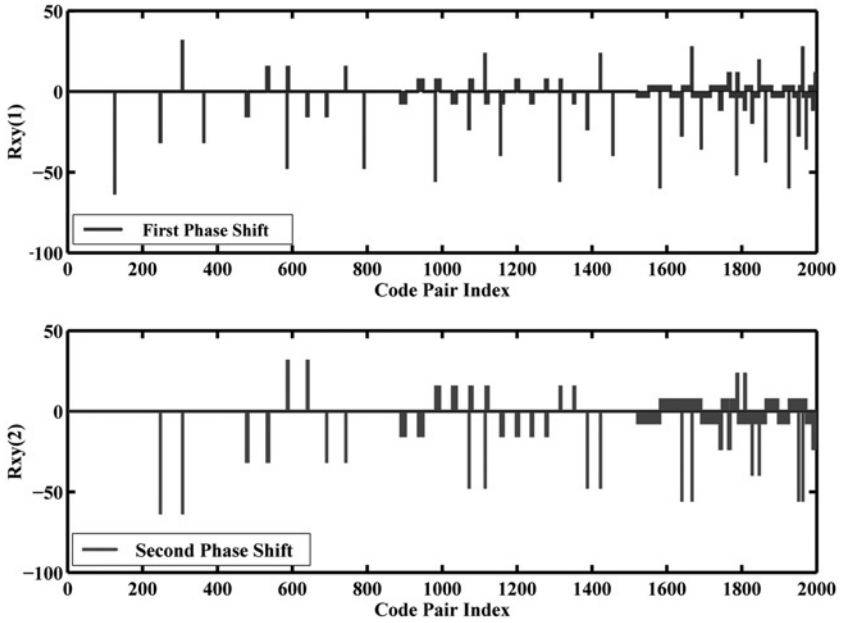

Fig. 2 *Cross-correlation of W(64,6) codes at the first and the second phase shifts*

Proof: The theorem can be proved using the mathematical induction as follows:

Statement: For each positive integer k, let $S(k)$ denote the statement: 'There exists a subset of $k+1$ codes among $\boldsymbol{W}$ $(2^k, k)$ denoted by $\widetilde{\boldsymbol{W}}^{(k)} \triangleq \left\{\widetilde{\boldsymbol{w}}_1^{(k)}, ..., \widetilde{\boldsymbol{w}}_{k+1}^{(k)}\right\}$ with zero cross-correlation for every value of the phase shift $\tau = 0, 1, ..., 2^k - 1$.'

Basis step: Clearly, the statement $S(k)$ holds when $k=1$, since two codes $\widetilde{\boldsymbol{w}}_1^{(1)} = [1, 1]$ and $\widetilde{\boldsymbol{w}}_2^{(1)} = [1, -1]$ generated from the Walsh–Hadamard matrix $\boldsymbol{H}_2$ have the following inner products (or equivalently cross-correlation) for $\tau = 0, 1$

$$R_{\widetilde{\boldsymbol{w}}_1^{(1)}\widetilde{\boldsymbol{w}}_2^{(1)}}(0) = [1, 1] \cdot [1, -1] = 0; \quad \text{Zero phase shift}$$

$$R_{\widetilde{\boldsymbol{w}}_1^{(1)}\widetilde{\boldsymbol{w}}_2^{(1)}}(1) = [1, 1] \cdot [-1, 1] = 0; \quad \text{First phase shift}$$

Inductive hypothesis: Suppose $S(k)$ is true for some values of $k \geq 1$ meaning that there are $k+1$ rows (or columns) of $\boldsymbol{H}_{2^k}$ which are orthogonal in all possible phase shifts $\tau = 0, 1, ..., 2^k - 1$. Let assume that $\widetilde{\boldsymbol{w}}_i^{(k)}(\xi)$ and $\widetilde{\boldsymbol{w}}_j^{(k)}(\xi')$ are two arbitrary distinct phase shifted codes selected from such $k+1$ rows of $\boldsymbol{H}_{2^k}$ with the arbitrary $0 \leq \xi, \xi' \leq 2^k - 1$. Since $S(k)$ is true, we have

$$\widetilde{\boldsymbol{w}}_i^{(k)}(\xi).\widetilde{\boldsymbol{w}}_j^{(k)}(\xi') = 0 \tag{4}$$

To prove that the statement $S(k+1)$ is true, it is necessary to find $k+2$ orthogonal phase shifted rows in $\boldsymbol{H}_{2^{k+1}}$. Clearly, the codeword $\widetilde{\boldsymbol{w}}_i^{(k)}$, $1 \leq i \leq 2^k$, in $\boldsymbol{H}_{2^k}$ appears in the first half part of $\boldsymbol{H}_{2^{k+1}}$ as $\widetilde{\boldsymbol{w}}_i^{(k+1)} = \left[\widetilde{\boldsymbol{w}}_i^{(k)}, \widetilde{\boldsymbol{w}}_i^{(k)}\right]$. For this case, the ξth phase shifted of $\widetilde{\boldsymbol{w}}_i^{(k+1)}$ would be as $\widetilde{\boldsymbol{w}}_i^{(k+1)}(\xi) = \left[\widetilde{\boldsymbol{w}}_i^{(k)}(\xi), \widetilde{\boldsymbol{w}}_i^{(k)}(\xi)\right]$.

Therefore from (3) and (4), we have the following zero cross-correlation result

$$\begin{aligned}&\widetilde{\boldsymbol{w}}_i^{(k+1)}(\xi).\widetilde{\boldsymbol{w}}_j^{(k+1)}(\xi') \\ &= \left[\widetilde{\boldsymbol{w}}_i^{(k)}(\xi), \widetilde{\boldsymbol{w}}_i^{(k)}(\xi)\right] \cdot \left[\widetilde{\boldsymbol{w}}_j^{(k)}(\xi'), \widetilde{\boldsymbol{w}}_j^{(k)}(\xi')\right] = 0\end{aligned} \tag{5}$$

where $1 \leq i, j \leq 2^k$ are the codewords indices belong to the first half part of $\boldsymbol{H}_{2^{k+1}}$. For the above result, $0 \leq \xi, \xi' \leq 2^k - 1$, while for $\xi, \xi' \geq 2^k$, the codewords are repeated periodically. According to the codewords indices $1 \leq i, j \leq 2^k$ and the result in (5), there exists a subset of $k+1$ (phase shifted) orthogonal codewords in the first half part of $\boldsymbol{H}_{2^{k+1}}$ belongs to $\widetilde{\boldsymbol{W}}^{(k+1)}$. We prove that the $(k+2)$th codeword in $\widetilde{\boldsymbol{W}}^{(k+1)}$ with the above cyclic orthogonal property is any arbitrary codeword $\boldsymbol{w}_j^{(k+1)}$ in the second half part of $\boldsymbol{H}_{2^{k+1}}$ (i.e. $2^k + 1 \leq j \leq 2^{k+1}$). To show that we denote (see (6))

with $1 \leq i \leq 2^k$, as the phase-shifted codeword in the first half part of $\boldsymbol{H}_{2^{k+1}}$ belong to $\widetilde{\boldsymbol{W}}^{(k+1)}$. For this case, $\widetilde{\boldsymbol{w}}_i^{(k+1)}(\xi) = \left[\widetilde{\boldsymbol{w}}_i^{(k)}(\xi), \widetilde{\boldsymbol{w}}_i^{(k)}(\xi)\right]$. In addition, we denote (see (7))

as an arbitrary phase-shifted codeword in the second half part of $\boldsymbol{H}_{2^{k+1}}$, where $0 \leq \xi, \xi' \leq 2^k - 1$. For this case, $\boldsymbol{w}_j^{(k+1)}(\xi') = \left[\boldsymbol{w}'_j, -\boldsymbol{w}'_j\right]$, where $\boldsymbol{w}'_j$ is defined as (see the equation at the bottom of the page)

Using (3), the cross-correlation value of the codewords $\widetilde{\boldsymbol{w}}_i^{(k+1)}(\xi)$ and $\boldsymbol{w}_j^{(k+1)}(\xi')$ would be as

$$\widetilde{\boldsymbol{w}}_i^{(k+1)}(\xi) \cdot \boldsymbol{w}_j^{(k+1)}(\xi') = \left[\widetilde{\boldsymbol{w}}_i^{(k)}(\xi), \widetilde{\boldsymbol{w}}_i^{(k)}(\xi)\right] \cdot \left[\boldsymbol{w}'_j, -\boldsymbol{w}'_j\right] = 0 \tag{8}$$

$$\begin{aligned}\widetilde{\boldsymbol{w}}_i^{(k+1)}(\xi) = \big[&w_{i,2^k-\xi+1} \quad w_{i,2^k-\xi+2} \quad \cdots \quad w_{i,2^k} \quad w_{i,1} \quad w_{i,2} \quad \cdots \quad w_{i,2^k-\xi} \\ &w_{i,2^k-\xi+1} \quad w_{i,2^k-\xi+2} \quad \cdots \quad w_{i,2^k} \quad w_{i,1} \quad w_{i,2} \quad \cdots \quad w_{i,2^k-\xi}\big]\end{aligned} \tag{6}$$

doi: 10.1049/iet-com.2012.0806

Therefore any arbitrary $w_j^{(k+1)}(\xi')$ in the second half part of $H_{2^{k+1}}$ with $2^k+1 \le j \le 2^{k+1}$ satisfies (8) and can be selected as $(k+2)$th element of $\tilde{W}(k+1)$. Thus, since there exists $k+2$ orthogonal phase-shifted rows in $H_{2^{k+1}}$, $S(k+1)$ is true and this completes the proof of the theorem. □

Remark 1: As explained in the proof of Theorem 1, among $k+1$ orthogonal phase shifted rows in H_{2^k}, 'there exists' one codeword in the second half part of this matrix that satisfies the zero cross-correlation rule with other elements of $\tilde{W}^{(k)}$ in each phase shift. In the following, we prove this statement that 'there is no two rows in the second half part of H_{2^k} with the above cyclic orthogonal property.'

Using the contradiction paradigm, suppose the above statement is false meaning that there exist two distinct rows $\tilde{w}_i^{(k)}$ and $\tilde{w}_j^{(k)}$ in the second half part of H_{2^k} with $2^{k-1}+1 \le i, j \le 2^k$, $i \ne j$, where for every values of ξ and ξ′

$$\tilde{w}_i^{(k)}(\xi) \cdot \tilde{w}_j^{(k)}(\xi') = 0 \tag{9}$$

Since (9) must be valid for every value of ξ and ξ′, we have (see (10))
The above equations set can be reformulated as the matrix form $Tx = \mathbf{0}$, where

$$T \triangleq \begin{bmatrix} w_{j,1} & w_{j,2} & \cdots & w_{j,2^{k-1}} \\ -w_{j,2^{k-1}} & w_{j,1} & \ddots & \vdots \\ \vdots & \ddots & \ddots & w_{j2} \\ -w_{j,2} & \cdots & -w_{j,2^{k-1}} & w_{j,1} \end{bmatrix} \tag{11}$$

is a Toeplitz or diagonal-constant matrix [24], and

$$x \triangleq \begin{bmatrix} w_{i,1} & w_{i,2} & \cdots & w_{i,2^{k-1}} \end{bmatrix}^{\mathrm{T}} \tag{12}$$

and $\mathbf{0} \triangleq [0, \ldots, 0]^{\mathrm{T}}$. There are two choices for the solution of $Tx = \mathbf{0}$. The first choice is $x = \mathbf{0}$; however, x is one row or one column of the matrix $H_{2^{k-1}}$ where the entries are belong to $\{-1, 1\}$, thus x cannot be an all-zeros vector. For the second choice, x can be in the null space of T meaning that each row of T multiplied with x is equal to zero. This implies that there are 2^{k-1} distinct rows in T orthogonal to x, while from the classical Walsh–Hadamard matrix $H_{2^{k-1}}$, there exist $2^{k-1}-1$ rows orthogonal to the vector x which is another row in $H_{2^{k-1}}$.

Remark 2: Now we are ready to prove that the 'exact' number of orthogonal phase shifted rows in H_{2^k} is $k+1$. To prove this statement, we use the result of Remark 1 where it is shown that there is only one orthogonal phase-shifted codeword in the second half part of H_{2^k} or equivalently in $\begin{bmatrix} H_{2^{k-1}} & -H_{2^{k-1}} \end{bmatrix}$, and the rest are in the first half part of H_{2^k}. It should be noted that $H_{2^{k-1}}$ can be rewritten as

$$H_{2^{k-1}} = \begin{bmatrix} H_2 \quad H_2 & \cdots & H_2 & H_2 \\ \underbrace{H_2 \quad -H_2}_{\text{2nd half part of } H_{2^2}} & \cdots & H_2 & -H_2 \\ & \vdots & & \\ \underbrace{H_{2^{k-3}} \quad -H_{2^{k-3}}}_{\text{2nd half part of } H_{2^{k-2}}} & & H_{2^{k-3}} & -H_{2^{k-3}} \\ \underbrace{H_{2^{k-2}} \quad -H_{2^{k-2}}}_{\text{2nd half part of } H_{2^{k-1}}} & & & \end{bmatrix} \tag{13}$$

According to the result of Remark 1, there exists exactly one orthogonal phase shifted codeword in each row of $H_{2^{k-1}}$ in (13) except the first row which yields $k-2$ Cyclic Orthogonal Walsh–Hadamard Codes (COWHCs). On the other hand, the first row of the matrix $H_{2^{k-1}}$ in (13) has been formed by H_2, which contains two orthogonal phase shifted codes. Thus, there are exactly k orthogonal phase shifted codes in the Walsh–Hadamard matrix $H_{2^{k-1}}$ or equivalently in the first half part of H_{2^k}. With emphasis on the result of Remark 1 for the second half part of H_{2^k}, it is concluded that the exact number of the orthogonal phase shifted codewords in H_{2^k} is $k+1$.

Remark 3: It is concluded from Theorem 1 that the necessary condition to avoid the MAI in the proposed uplink femtocell system is to choose the code length $N = 2^k$ such that $K \le k+1$. We call the subset $\tilde{W}^{(k)}$ as the COWHCs in the proposed asynchronous CDMA-based femto system. Surprisingly, the MAI imposed in the second term of (2) is completely cancelled through utilising the preassigned COWHCs. Fig. 3 illustrates a tree diagram of COWHCs for $1 \le k \le 6$. It is seen that the number of COWHCs subsets for every value of k, denoted by $\mathcal{O}_k$, is not unique and is obtained as

$$\mathcal{O}_k = \prod_{\ell=1}^{k} 2^{\ell-1}, \qquad k \ge 1 \tag{14}$$

We use the COWHCs subsets to study the link-level (BER)

$$w_j^{(k+1)}(\xi') = \big[-w_{j,2^k-\xi'+1} \quad -w_{j,2^k-\xi'+2} \quad \cdots \quad -w_{j,2^k} \quad w_{j,1} \quad w_{j,2} \quad \cdots \quad w_{j,2^k-\xi'} \\ w_{j,2^k-\xi'+1} \quad w_{j,2^k-\xi'+2} \quad \cdots \quad w_{j,2^k} \quad -w_{j,1} \quad -w_{j,2} \quad \cdots \quad -w_{j,2^k-\xi'}\big] \tag{7}$$

$$w'_j = \big[-w_{j,2^k-\xi'+1} \quad -w_{j,2^k-\xi'+2} \quad \cdots \quad -w_{j,2^k} \quad w_{j,1} \quad w_{j,2} \quad \cdots \quad w_{j,2^k-\xi'}\big]$$

$$\begin{cases} w_{i,1}w_{j,1} + w_{i,2}w_{j,2} + \cdots + w_{i,2^{k-1}}w_{j,2^{k-1}} = 0, & \text{for } \xi = 0, \xi' = 0 \\ -w_{i,1}w_{j,2^{k-1}} + w_{i,2}w_{j,1} + \cdots + w_{i,2^{k-1}}w_{j,(2^{k-1}-1)} = 0, & \text{for } \xi = 0, \xi' = 1 \\ & \vdots \\ -w_{i,1}w_{j,2} - w_{i,2}w_{j,3} + \cdots + w_{i,2^{k-1}}w_{j,1} = 0, & \text{for } \xi = 0, \xi' = 2^{k-1}-1 \end{cases} \tag{10}$$

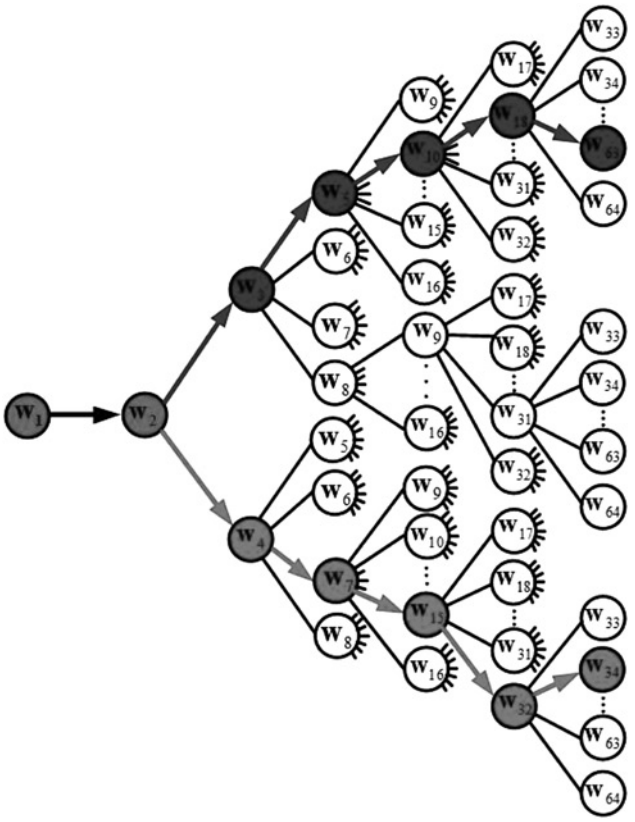

Fig. 3 *Tree-diagram of cyclic orthogonal Walsh–Hadamard codes for $1 \leq k \leq 6$*

performance of the proposed asynchronous femtocell system in the next section.

4 Numerical results

To demonstrate the effectiveness of the COWHCs subset for the MAI suppression in the proposed asynchronous CDMA-based femtocell model in Section 2, a set of experiments are conducted to examine the link-level (BER) performance of the system in an AWGN/fading channel. Towards this goal in this section, we present some numerical results to compare the performance of our COWHC-based scheme with that of conventional spreading codes such as Gold codes [25]. In addition, the simulation setup considers a channel estimator in a multipath-fading environment using Kalman filtering [26]. We assume a CDMA-based femtocell system consisting of $K = 7$ wireless devices communicating to the femto access point *AP*. It should be noted that in reality, the number of active users in a femtocell is a random variable with the Poisson distribution. Owing to the dependency between the length of COWHCs and the number of users in a femtocell, as proved in Theorem 1, the number of active users K is considered as a deterministic variable. The femto devices are assumed to be uniformly distributed inside each femtocell. It should be noted that in our femto model, we assume that the time-line of all asynchronous users should be aligned chip-by-chip, that is, the minimum time shift should be a chip duration. Our simulation setup utilises the well-known maximal-ratio combining (MRC) for the CDMA rake receiver [27] to evaluate the performance of the proposed algorithm. The rake receiver is designed to optimally detected a DS-CDMA signal transmitted over a dispersive multipath channel. The cross-layer and the co-layer interference can be negligible using interference cancellation methods. It is clear that in the presence of the interference, the proposed cyclic orthogonal codes have better performance than other spreading codes such the Gold codes. Thus for simplicity, we focus on the interference caused in the uplink communication from the interferer inside one femtocell.

Our simulation results are based on the MC technique that is applied to the estimation of the BER. For the MC simulations, we perform the following steps:

Step 1: Generate a binary data stream with the length N for each user. To reach a lower order of BER such as 10^{-3}, it is necessary that $N \geq 10\,000$.
Step 2: Modulate the input data by the binary phase shift keying (BPSK).
Step 3: Spread the binary sequence using the conventional Walsh–Hadamard, cyclic orthogonal Walsh–Hadamard and Gold codes.
Step 4: Send the spread data through the AWGN/Rayleigh-fading channel.
Step 5: Despread the received signal for a specific user.

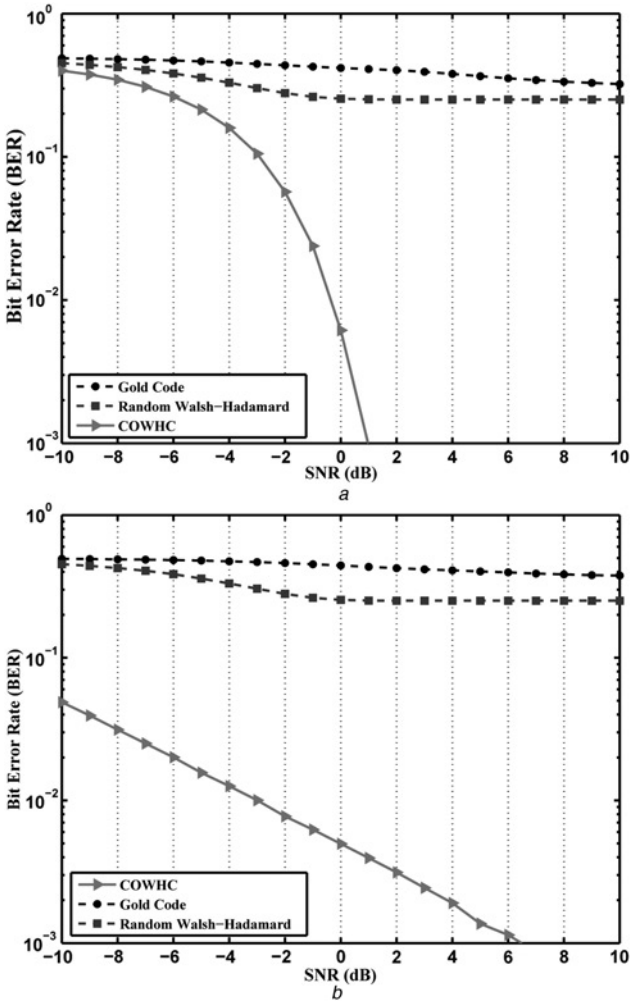

Fig. 4 *Link-level (BER) performance against SNR for various spreading codes with spreading factor $N = 64$ in a femtocell with $K = 7$ for*

a AWGN and
b Rayleigh-fading channel

doi: 10.1049/iet-com.2012.0806

It should be noted that the effect of the asynchronous users appears in Step 4 and this event causes an error in Step 5. The above MC simulation is run over a range of E_b/N_0 values using the same value of N for each E_b/N_0 that results in an estimated value of the BER.

Presented in Fig. 4, we evaluate the link-level (BER) of the proposed COWHCs with $N = 2^k = 64$ for different signal-to-noise ratios (SNRs) for the current CDMA-based femtocell model with $K = k + 1 = 7$, where the received signals at the *AP* are corrupted with an AWGN and flat fading. The SNR level is assumed to vary from -10 dB (low SNR regime) to +10 dB (high SNR regime) with 1 dB as a step size. The BER of the COWHCs is compared with that of the Gold codes [25] and the classical Walsh–Hadamard codes (non-cyclic codes), where we randomly select $K = 7$ codes among the Hadamard matrix $\boldsymbol{H}_{26}$ in each iteration. Surprisingly, it is evident as shown in Fig. 4 that there exists a magnificent performance gain for the utilised COWHCs as the SNR increases for both the AWGN and the fading channels. This performance gain (high reliability) is achieved due to the cyclic orthogonality property of the COWHCs as the MAI is mitigated and less bits are decoded in error at the *AP*.

To make a fair comparison between our proposed COWHCs scheme and previous works, we use the time hopping (TH) spread spectrum technique in [28] used in femtocells. In the proposed TH-based scenario in [28], each transmitter sends N_f pulses for each bit. The bit duration is divided into N_f frames and exactly one pulse is sent in each frame. The exact position of the pulse in each frame depends on the pseudo-random data and the desired transmitter. The pseudorandom sequence is a sequence of integer numbers between 0 and $N_h - 1$ where N_h is the number of chips in each frame. This sequence changes randomly the position of pulses in each frame. In each frame, this integer is multiplied by T_c where T_c is the chip duration. To ensure that only one pulse is sent in each frame, it is necessary that $N_h T_c \leq T_f$, where T_f is the frame duration. Fig. 5 presents the BER performance comparison between our proposed COWHCs and the TH-based technique in [28]. As seen in Fig. 5, the BER of our proposed COWHCs is less than the scheme in [28] for every value of the processing gain N and for the first and the second phase-shifted.

So far, we assumed that the cross-layer interferences from different sources are controlled by the orthogonal signalling in the network. In the following, we relax this assumption and investigate the BER performance of the proposed COWHCs under the existence of the cross-layer interference. For this purpose, we present a comparison between two scenarios in Fig. 6 as follows:

(i) The FAP receives the interfere signal from femto user equipments (fues) (known as the co-layer interference).
(ii) The FAP is affected by the interferer fues as well as the cross-layer interference caused by macro user equipments (mues) that use non-COWHCs.

As depicted in the simulation results in Fig. 6, the proposed scheme with the COWHCs has a significant improvement on the BER performance in both scenarios (i) and (ii). This implies that our proposed COWHCs are applicable in real femto systems that suffer from both cross-layer and co-layer interferences.

To complete the evaluation of our proposed scheme, we examine the BER performance of the COWHCs in the proposed femtocell model where the channel taps α_{ij}'s are estimated using Kalman filtering. In the Kalman-based estimation, a known pilots sequence is transmitted simultaneously along with the other channels signals to perform the estimation. These channels that are parallel with each others, behave as the interfering signals, however by spreading the pilot and the data with COWHCs, the interference from the other parallel channels will be suppressed. Recalling α_{ij} (n) denotes the jth channel tap coefficient between the femto node U_i and the *AP* at time slot n, and defining the random vector $\boldsymbol{h}_n^{(i)} \triangleq [\alpha_{i1}(n), \ldots, \alpha_{iL}(n)]^T$, the vector $\boldsymbol{h}_n^{(i)}$ is modelled as a multichannel autoregressive (AR) random process of order q [29]

$$\boldsymbol{h}_n^{(i)} = \sum_{\ell=1}^{q} \boldsymbol{A}(\ell)\boldsymbol{h}_{n-1}^{(i)} + \boldsymbol{u}_{n-1} \tag{15}$$

where the $L \times L$ matrices $\mathbf{A}(\ell)$'s, $\ell = 1, \ldots, q$, are the solutions of the q Yule–Walker equations, and the entries of the vector $\boldsymbol{u}_{n-1}$ are independent and identically distributed circular complex Gaussian random variables. Dropping the

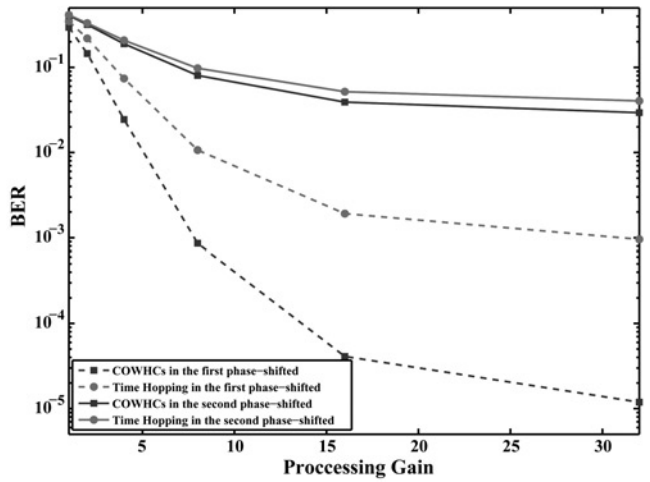

Fig. 5 *BER against processing gain for the proposed COWHCs and time hopping-based technique in [28]*

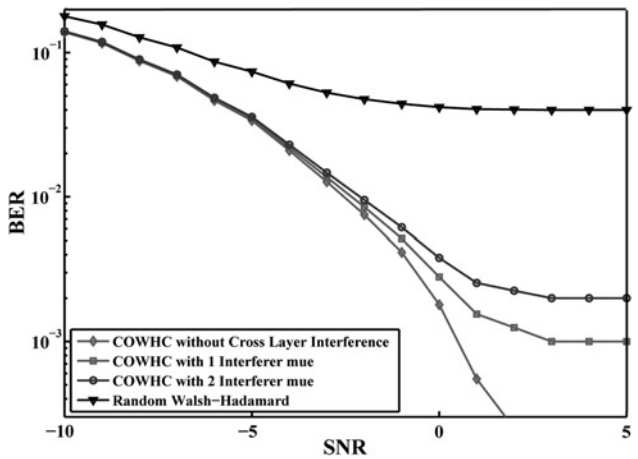

Fig. 6 *BER against SNR in the presence and absence of the interferers mues and for K = 7*

superscript (i) in (15) for ease of our analysis, we define the $Lq \times 1$ vector $\boldsymbol{x}_n \triangleq [\boldsymbol{h}_n^{\mathrm{T}}, \boldsymbol{h}_{n-1}^{\mathrm{T}}, ..., \boldsymbol{h}_{n-q+1}^{\mathrm{T}}]^{\mathrm{T}}$ to rewrite (15) as

$$\boldsymbol{x}_{n+1} = \boldsymbol{F}\boldsymbol{x}_n + \boldsymbol{G}\boldsymbol{u}_n \tag{16}$$

where $\boldsymbol{F}$ is an $Lq \times Lq$ state transition matrix given by

$$\boldsymbol{F} = \begin{bmatrix} \boldsymbol{A}(1) & \boldsymbol{A}(2) & \cdots & \boldsymbol{A}(q) \\ \boldsymbol{I}_{L\times L} & \boldsymbol{0}_{L\times L} & \cdots & \boldsymbol{0}_{L\times L} \\ \vdots & \ddots & \ddots & \vdots \\ \boldsymbol{0}_{L\times L} & \cdots & \boldsymbol{I}_{L\times L} & \boldsymbol{0}_{L\times L} \end{bmatrix}$$

and

$$\boldsymbol{G} = \begin{bmatrix} \boldsymbol{I}_{L\times L} \\ \boldsymbol{0}_{(q-1)L\times L} \end{bmatrix}$$

For our simulation, we consider the pilot-assisted channel estimation technique, where the approach makes the AP to estimate the channel taps α_{ij}'s. In the following, we use the Kalman filter-based channel estimation algorithm to track a simple Gauss–Markov channel. Defining $\boldsymbol{s}_n = [s(n), s(n-1), \ldots, s(n-L+1)]^{\mathrm{T}}$, the derivation of Gauss–Markov equations is performed by collecting q consecutive realisations of the received data into a column vector

$$\boldsymbol{y}_n = [y(n), y(n-1), \ldots, y(n-q+1)]^{\mathrm{T}} = \boldsymbol{H}\boldsymbol{x}_n + \boldsymbol{v}_n \tag{17}$$

where $\boldsymbol{H}$ is an $q \times Lq$ diagonal measurement matrix defined as

$$\boldsymbol{H} = \begin{bmatrix} \boldsymbol{s}_n & \boldsymbol{0}_{1\times L} & \cdots & \boldsymbol{0}_{1\times L} \\ \boldsymbol{0}_{1\times L} & \boldsymbol{s}_{n-1} & \cdots & \boldsymbol{0}_{1\times L} \\ \vdots & \ddots & \ddots & \vdots \\ \boldsymbol{0}_{1\times L} & \cdots & \boldsymbol{0}_{1\times L} & \mathbf{s}_{n-q+1} \end{bmatrix}$$

and $\boldsymbol{v}_{\mathrm{n}}$ is the measurement noise vector with the covariance matrix $\boldsymbol{R}_n \triangleq \mathbb{E}\{\boldsymbol{v}_n \cdot \boldsymbol{v}_n^H\}$. Using (16) and (17) as the desired state and measurement equations, and the square root covariance filter algorithm, the Kalman filtering is implemented by the following update and prediction formulas [30]:

Step 1 (A priori estimation and measurement stage along with the estimation update): (see (18))

where $\tilde{\boldsymbol{T}}$ is a unitary matrix, $\boldsymbol{Q}_k = \boldsymbol{Q}_k^{1/2}\left[\boldsymbol{Q}_k^{1/2}\right]'$, $\boldsymbol{R}_k = \boldsymbol{R}_k^{1/2}\left[\boldsymbol{R}_k^{1/2}\right]'$, $\sum_{k|k-1} = \boldsymbol{\delta}_k\boldsymbol{\delta}'_k$, and (see (19))

$$\widetilde{\boldsymbol{K}}_k = \sum\nolimits_{k|k-1}\boldsymbol{H}_k\left[\left(\boldsymbol{H}'_k\sum\nolimits_{k|k-1}\boldsymbol{H}_k + \boldsymbol{R}_k\right)^{-(1/2)}\right]' \tag{20}$$

Step 2 (Estimation of the noise and measurement covariance matrix):

$$\hat{\boldsymbol{u}}_k = \hat{\boldsymbol{h}}_{k|k} - \boldsymbol{F}_k\hat{\boldsymbol{h}}_{k-1|k} \tag{21}$$

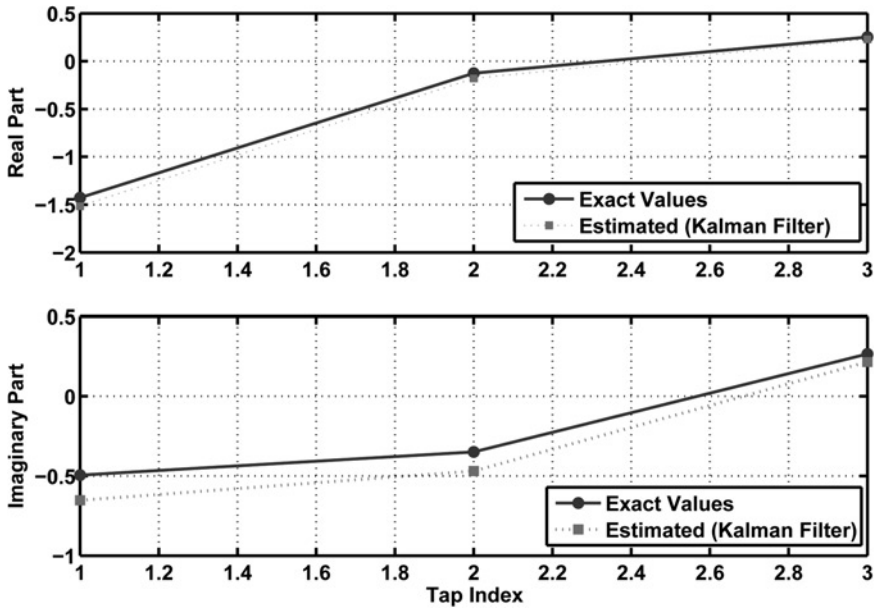

Fig. 7 *Exact values of the real and the imaginary parts of tap coefficients $\alpha_{\ell j}$ compared with the estimated ones obtained from the MRC-based Kalman filtering for $L = 3$*

$$\begin{bmatrix} \left[\left(\boldsymbol{H}'_k\sum_{k|k-1}\boldsymbol{H}_k + \boldsymbol{R}_k\right)^{-\frac{1}{2}}\right]' & \tilde{\boldsymbol{K}}'_k\boldsymbol{F}'_k \\ \boldsymbol{0} & \delta'_{k|k-1} \\ \boldsymbol{0} & \boldsymbol{0} \end{bmatrix} = \tilde{\mathbf{T}}\begin{bmatrix} \left[\boldsymbol{R}_k^{\frac{1}{2}}\right]' & \boldsymbol{0} \\ \delta'_{k|k-1}\boldsymbol{H}_k & \delta'_{k|k-1}\boldsymbol{F}'_k \\ \boldsymbol{0} & \left[\boldsymbol{Q}_k^{\frac{1}{2}}\right]'\boldsymbol{G}'_k \end{bmatrix} \tag{18}$$

$$\hat{\boldsymbol{x}}_{k+1|k} = \boldsymbol{F}_k\left[\hat{\boldsymbol{x}}_{k|k-1} + \widetilde{\boldsymbol{K}}_k\left(\boldsymbol{H}'_k\sum\nolimits_{k|k-1}\boldsymbol{H}_k + \boldsymbol{R}_k\right)\right]^{-(1/2)}\left(\boldsymbol{y}_k - \boldsymbol{H}'_k\hat{\boldsymbol{x}}_{k|k-1}\right) \tag{19}$$

doi: 10.1049/iet-com.2012.0806

$$\boldsymbol{Q}_k = \frac{1}{M+1} \sum_{\ell=k-1-M}^{k-1} \hat{\boldsymbol{u}}_\ell \hat{\boldsymbol{u}}'_\ell \tag{22}$$

$$\hat{\boldsymbol{v}}_k = \boldsymbol{z}_k - \boldsymbol{H}'_k \hat{\boldsymbol{h}}_{k|k-1} \tag{23}$$

$$\boldsymbol{R}_k = \frac{1}{M+1} \sum_{\ell=k-1-M}^{k-1} \hat{\boldsymbol{v}}_\ell \hat{\boldsymbol{v}}'_\ell \tag{24}$$

where the averaging in (22) and (24) is performed over $M+1$ estimated data.

Fig. 7 compares the exact values of the real and the imaginary parts of tap coefficients $\alpha_{\ell j}$ with the estimated $\hat{\alpha}_{\ell j}$ obtained from the described MRC-based Kalman filtering for $L=3$. Interestingly, we see from Fig. 7 that the estimated channel tap $\hat{\alpha}_{\ell j}$ obtained from the Kalman filtering is close to the real ones. Taking the above considerations into account and recalling from (2), let $\hat{s}_\ell(n)$ denote the nth estimated data symbol for the ℓth user using multipath, and let $\hat{\boldsymbol{h}}_n^{(\ell)} \triangleq \left[\hat{\alpha}_{\ell 1}(n), \ldots, \hat{\alpha}_{\ell L}(n)\right]$ denote the estimated channel vector for the ℓth user. For this case, the MRC rake receiver output for the nth data symbol of user ℓ is given by

$$\hat{s}_\ell(n) = \sum_{j=1}^{L} \hat{\alpha}^*_{\ell j}(n) s_\ell(n-\tau_{\ell j}) w_\ell^2 + \sum_{\substack{i=1 \\ i\neq\ell}}^{K} \sum_{j=1}^{L} \hat{\alpha}^*_{ij}(n) s_i\left(n-\tau_{ij}\right) w_i w_\ell + w_\ell z(n), \quad \ell = 1, \ldots K \tag{25}$$

where the second term would be zero because of the orthogonality of the utilised Walsh–Hadamard codes. Now, we are ready to evaluate the robustness of the proposed COWHCs in an AWGN/fading channel model with the MRC-based rake receiver in terms of the link-level BER (as depicted in Fig. 8) for the following two scenarios:

(i) The *AP* deploys a maximum ratio combiner and uses the exact values of $\alpha_{\ell j}$'s, $j=1, \ldots, L$. In addition, the delay parameters $\tau_{\ell j}$'s are known in advance for the rake receiver. We also use the classical Walsh–Hadamard codes with $N=64$ for this synchronous rake receiver.
(ii) The *AP* uses the MRC-based rake receiver where only the estimated channel taps $\hat{\alpha}_{\ell j}$'s (obtained from Kalman filtering) are utilised with no requirement of knowing the delay $\tau_{\ell j}$'s at the rake receiver in the *AP*. For this scenario, we utilise the COWHCs with $N=64$.

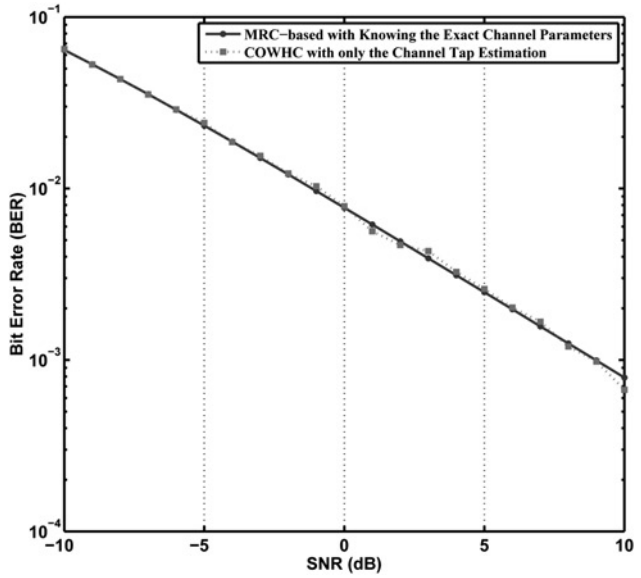

Fig. 8 *BER performance against SNR for the MRC-based Kalman filtering and without channel estimation in a femtocell with $K=7$ and Rayleigh-fading channel model*

As shown in Fig. 8, we see that the performance of the second scenario where the Kalman filtering is utilised for the channel estimation is matched to the first one with real values of the multipath-fading channel. This result comes from the asynchronicity and the cyclic orthogonality of the utilised COWHCs where the *AP* does not need any information about the delay $\tau_{\ell j}$ for the rake receiver and the zero cross correlation is achieved with the utilised COWHCs. This property reduces the complexity of the rake receiver at the *AP* in an asynchronous femtocell system.

5 Conclusion

The asynchronous nature of CDMA-based femtocell systems and the non-orthogonality of spreading codes produce multiple access interference at the femto access point which contributes to decoding errors and the lower link reliability. In this paper, we presented an augmentation protocol for the physical layer of the CDMA2000 femtocell standard with focus on the MAI suppression. The proposed scheme uses a unique set of cyclic orthogonal binary codes to eliminate the MAI caused by packet collisions. The cyclic orthogonality property of COWHCs was studied and analysed. This property ensures that the time and data rate asynchronicity of active nodes in a femtocell produces a zero MAI situation at the FAP. The work investigates the optimality and the effectiveness of such codes in femtocells from the link BER performance in a practical Rayleigh-fading environment and AWGN. Theoretical findings are verified by simulation evaluations and it was shown numerically a significant improvement in the performance of the proposed scheme when compared with conventional non-cyclic orthogonal codes such as classical Walsh–Hadamard and Gold codes in a Rayleigh-fading channel. The cyclic orthogonality property of COWHCs in the interference mitigation yields an increase in the femtocell capacity as well. We have also used Kalman filtering at the FAP for the channel estimation. Our simulation results show that the COWHCs can reduce the complexity of the rake receiver with the Kalman filtering process when compared with the conventional MRC rake receiver in an asynchronous femtocell system.

6 References

1 Claussen, H., Ho, L.T., Samuel, L.G.: 'An overview of the femtocell concept', *Bell Labs Tech. J.*, 2008, **13**, (1), pp. 221–246
2 Chandrasekhar, V., Andrews, J.G., Gatherer, A.: 'Femtocell networks: a survey', *IEEE Commun. Mag.*, 2008, **46**, (9), pp. 59–67
3 Xia, P., Chandrasekhar, V., Andrews, J.G.: 'Open vs. closed access femtocells in the uplink', *IEEE Trans. Wirel. Commun.*, 2010, **9**, (12), pp. 3798–3809

4 Kim, Y., Lee, S., Hong, D.: 'Performance analysis of two-tier femtocell networks with outage constraints', *IEEE Trans. Wirel. Commun.*, 2010, **9**, (9), pp. 2695–2700

5 Jacob, P., Madhukumar, A.S.: 'Interference reduction through femto-relays', *IET Commun.*, 2012, **6**, (14), pp. 2208–2217

6 Oh, D.-C., Lee, H.-C., Lee, Y.-H.: 'Power control and beamforming for femtocells in the presence of channel uncertainty', *IEEE Trans. Veh. Technol.*, 2011, **60**, (6), pp. 2545–2554

7 Park, S., Seo, W., Kim, Y., Lim, S., Hong, D.: 'Beam subset selection strategy for interference reduction in two-tier femtocell networks', *IEEE Trans. Wirel. Commun.*, 2010, **9**, (11), pp. 3440–3449

8 Jo, H.-S., Mun, C., Moon, J., Yook, J.-G.: 'Interference mitigation using uplink power control for two-tier femtocell networks', *IEEE Trans. Wirel. Commun.*, 2009, **8**, (10), pp. 4906–4910

9 Yun, J.-H., Shin, K.G.: 'Adaptive interference management of OFDMA femtocells for co-channel deployment', *IEEE J. Sel. Areas Commun.*, 2011, **29**, (6), pp. 1225–1241

10 Chang, C.-W.: 'An interference-avoidance code assignment strategy for the hierarchical two-dimensional-spread MC-DS-CDMA system: a prototype of cognitive radio femtocell system', *IEEE Trans. Veh. Technol.*, 2012, **61**, (1), pp. 166–184

11 Sun, Y., Jover, R.P., Wang, X.: 'Uplink interference mitigation for OFDMA femtocell networks', *IEEE Trans. Wirel. Commun.*, 2012, **11**, (2), pp. 614–625

12 Mhiri, F., Sethom, K., Bouallegue, R.: 'A survey on interference management techniques in femtocell self-organizing networks', *J. Netw. Comput. Appl.*, 2013, **36**, (1), pp. 58–65

13 Ĺopez-P´erez, D., Valcarce, A., de la Roche, G., Zhang, J.: 'OFDMA femtocells: a roadmap on interference avoidance', *IEEE Commun. Mag.*, 2009, **47**, (9), pp. 41–48

14 Wang, L.-C., Lee, C., Huang, J.-H.: 'Distributed channel selection principles for femtocells with two-tier interference'. Proc. 71st IEEE Vehicular Technology Conf. (VTC), Taipei, Taiwan, May 2010, pp. 1–5

15 Ngo, D.T., Le, L.B., Le-Ngoc, T., Hossain, E., Kim, D.I.: 'Distributed interference management in two-tier CDMA femtocell networks', *IEEE Trans. Wirel. Commun.*, 2012, **11**, (3), pp. 979–989

16 Dixon, R.C.: 'Spread spectrum systems with commercial applications' (John Wiely and Sons, New York, 1994), 3th edn.

17 Humblet, P., Raghothaman, B., Srinivas, A., Balasubramanian, S., Patel, C., Yavuz, M.: 'System design of CDMA2000 femtocells', *IEEE Commun. Mag.*, 2009, **47**, (9), pp. 92–100

18 Lim, T.J., Rasmussen, L.K., Sugimoto, H.: 'An asynchronous multiuser CDMA detector based on the Kalman filter', *IEEE J. Sel. Areas Commun.*, 1998, **16**, (9), pp. 1711–1722

19 Parkvall, S.: 'Variability of user performance in cellular DS-CDMA-long versus short spreading sequences', *IEEE Trans. Commun.*, 2000, **48**, (7), pp. 1178–1187

20 Horadam, K.J.: 'Hadamard matrices and their applications' (Princeton University Press, 2007, 1st edn.)

21 Abouei, J.: 'Analysis of orthogonal codes and their applications in cellular communication systems', MSc thesis, Isfahan University of Technology, Iran, 1996

22 Abouei, J.: 'A set of cyclic orthogonal codes acquired from Walsh–Hadamard matrix'. Proc. 34th International Mathematics Conf., Shahrood, Iran, Sept. 2003, pp. 1–4

23 Tawfiq, A., Abouei, J.: 'Cyclic orthogonal codes in CDMA-based asynchronous wireless body area networks'. Proc. IEEE International Conf. on Acoustics, Speech and Signal Processing (ICASSP'12), Kyoto, Japan, March 2012, pp. 1593–1596

24 Bottcher, A., Grudsky, S.: 'Toeplitz matrices, asymptotic linear algebra, and functional analysis' (Hindustan Book Agency, New Delhi (India), 2000), 1st edn.

25 Gold, R.: 'Optimal binary sequences for spread spectrum multiplexing', *IEEE Trans. Inf. Theory*, 1967, **13**, (4), pp. 619–621

26 Teng, L.J., Yao, M.: 'The Kalman filter as the optimal linear minimum mean-squared error multiuser CDMA detector', *IEEE Trans. Inf. Theory*, 2000, **46**, (7), pp. 2561–2566

27 Goldsmith, A.: 'Wireless communications' (Cambridge University Press, 2005), 1st edn

28 Chandrasekhar, V., Andrews, J.G.: 'Uplink capacity and interference avoidance for two-tier femtocell networks', *IEEE Trans. Wirel. Commun.*, 2009, **8**, (7), pp. 3498–3509

29 Baddour, K.E., Beaulieu, N.C.: 'Autoregressive modeling for fading channel simulation', *IEEE Trans. Wirel. Commun.*, 2005, **4**, (4), pp. 1650–1662

30 Verhaegen, M., Van Dooren, P.: 'Numerical aspects of different Kalman filter implementations', *IEEE Trans. Autom. Control*, 1986, **31**, (10), pp. 907–917

doi: 10.1049/iet-com.2012.0806